

Cite this article as: Zhao Guoqi, Tian Sugui, Liu Lirong, et al. Deformation Mechanism of Single-Crystal Nickel-based Superalloys During Ultra-High-Temperature Creep[J]. Rare Metal Materials and Engineering, 2022, 51(01): 52-59.

ARTICLE

Deformation Mechanism of Single-Crystal Nickel-based Superalloys During Ultra-High-Temperature Creep

Zhao Guoqi^{1,2}, Tian Sugui¹, Liu Lirong¹, Tian Ning², Jin Fangwei²

¹ School of Materials Science and Engineering, Shenyang University of Technology, Shenyang 110870, China; ² School of Mechanical Engineering, Guizhou University of Engineering Science, Bijie 551700, China

Abstract: The creep behavior and deformation mechanism of the nickel-based single-crystal superalloy containing 6wt% Re and 5wt% Ru at ultra-high temperatures were studied via microstructure observation and creep property analysis. The results show that under the condition of 1160 °C/120 MPa, the Ni-based superalloy has a creep life of 206 h. During the steady state creep period, the deformation mechanism is dominated by dislocation glide in the γ matrix and dislocation climb over the γ' raft phases. The refractory elements dissolved in the γ matrix can improve the resistance to dislocation movement. In the late creep stage, the cross-slip occurs from $\{111\}$ plane to the $\{100\}$ plane with the dislocations used for shearing the γ' phase, and then the Kear-Wilford (K-W) dislocation locks are formed. A large number of K-W dislocation locks can inhibit the dislocation glide and cross-slip, thus improving the creep resistance and reducing the strain rate for Ni-based superalloys. In the late creep stage, the cross-slip dislocations are initiated to twist the γ'/γ raft phases, and the crack initiation and propagation occur in the γ'/γ interfaces until fracture. These phenomena are the damage and fracture features of the Ni-based superalloys. The Ru atoms dissolved in the γ' phase can replace the Al atoms. When Ru, Re, and W atoms react in the Ni-based superalloy, more Re and W atoms can be dissolved into the γ' phase, which reduces the element diffusion rate and hinders the dislocation movement, thereby retaining more K-W dislocation locks and excellent creep resistance of Ni-based superalloys at ultra-high temperatures.

Key words: single-crystal nickel-based superalloy; 6%Re-5%Ru; creep; deformation mechanism; K-W dislocation lock

With increasing the power and thrust-to-weight ratio of aeroengines, the materials for the hot-end parts of the engine are required for high-temperature bearing capacities^[1-3]. The addition of refractory elements, such as W, Mo, Ta, Re, and Ru, can enhance the temperature bearing capacity of alloys. When the Re content increases to 3wt% and 6wt%, the temperature bearing capacity of the alloys can be increased by 30 and 60 °C, respectively^[4,5]. The specific Re content of 3wt% and 6wt% is the main composition feature of the second-generation and third-generation nickel-based single-crystal superalloys.

Re has a larger atomic radius and smaller diffusion coefficient than other refractory elements do. During creep, Re can maintain the structural stability and decrease the diffusion rates of other elements in the alloy^[6]. In particular,

the heavy atoms Re and W are precipitated near the γ'/γ interface, which results in the lattice distortion and hindrance of dislocation movement, thereby improving the creep resistance of the alloys^[7]. However, with increasing the Re content, more topologically close-packed (TCP) phases are precipitated. Once the TCP phase is precipitated from the alloys, the crack initiation and propagation occur easily in the area next to TCP phase during creep, so the creep performance can be greatly reduced^[8]. The addition of Ru in Re-containing alloys can inhibit the precipitation of TCP phase^[9] and greatly enhance the high-temperature creep properties^[10-12]. In particular, the fourth-generation single-crystal nickel-based superalloys with 2wt%~4wt% Ru and 5wt%~6wt% Re show excellent mechanical properties and creep resistances at about 1100 °C^[13]. As the Re/Ru content increases, the temperature

Received date: April 09, 2021

Foundation item: Science and Technology Foundation Project of Guizhou Province (qiankehejichu[2020]1Y198, qiankehezicheng[2019]2870); Projects of Liaoning Natural Science Foundation (2020-MS-212); Science and Technology Project of Bijie City (bikehezi[2019]2); Characteristic Key Laboratory of University of Guizhou Province (qianjiaoheKYzi[2019]053)

Corresponding author: Tian Sugui, Ph. D., Professor, School of Materials Science and Engineering, Shenyang University of Technology, Shenyang 110870, P. R. China, Tel: 0086-24-25496301, E-mail: lrlu@sut.edu.cn

Copyright © 2022, Northwest Institute for Nonferrous Metal Research. Published by Science Press. All rights reserved.

bearing capacity of the alloys are greatly improved.

The single-crystal nickel-based superalloys have good high-temperature mechanical and creep properties with abnormal yield behavior of Ni₃Al phase^[14], because during the thermal deformation, the cross-slip from the {111} plane to the {100} plane occurs with activated dislocations, forming the Kear-Wilford (K-W) dislocation locks with a non-planar core structure. Because K-W dislocation locks can hinder the dislocation glide and cross-slip, the deformation resistance of superalloys is greatly improved^[15]. However, as the temperature further increases, the dislocation in the K-W dislocation lock can be reactivated, causing the dislocation glide on the {111} plane again and breaking the K-W dislocation lock^[16]. The addition of Re/Ru can increase the peak temperature of the abnormal yield behavior^[17]. Only a small number of K-W dislocation locks are formed and retained in the single-crystal alloy containing 4.5wt% Re during creep at 1100 °C. More K-W dislocation locks are retained in the single-crystal alloy after adding 3wt% Ru^[18], thereby enhancing the creep properties at high temperatures. However, with further increasing the Re/Ru content, it is still not clear whether the K-W dislocation locks are formed or retained during the ultra-high-temperature creep. It is reported that in the late creep stage of an alloy containing Re/Ru, the dislocations used for shearing the γ' phase can be decomposed to form the incomplete dislocation+superlattice intrinsic stacking fault (SISF) configuration or the incomplete dislocation+anti-phase boundary (APB) configuration^[19,20]. However, the creep behavior and deformation mechanisms of single-crystal nickel-based superalloys containing 6wt% Re and 5wt% Ru at ultra-high-temperatures are still unclear.

In this research, the single-crystal nickel-based superalloys containing 6wt% Re and 5wt% Ru were prepared to examine the creep behavior and deformation mechanisms at ultra-high temperatures. The creep tests and microstructure observations of the Ni-based superalloys under the condition of 1160 °C/120 MPa were conducted, and the dislocation configuration was also analyzed.

1 Experiment

The [001]-oriented nickel-based single-crystal superalloys with the dimension of 16 mm×190 mm were prepared via crystal selection method in a ZGD-2 vacuum directional solidification furnace under a high temperature gradient. The nominal chemical composition of the Ni-based superalloy was Ni-Al-Ta-Cr-Co-Mo-W-6.0wt% Re-5.0wt% Ru, namely 6%Re-5%Ru Ni-based superalloy. The orientation difference of all the specimens is within 7° from the [001] orientation. It is reported that the continuous heating and solution treatment of the alloy in the temperature range from the solid solution line to the solidus line can improve the homogeneity of the alloy and avoid the formation of incipient melting phase^[21]. Therefore the heat treatment was as follows: 1300 °C-2 h+1310 °C-6 h+1315 °C-10 h+1323 °C-10 h+1328 °C-10 h+1332 °C-5 h+air cooling+1180 °C-4 h+air cooling+870 °C-24 h+air cooling.

After heat treatment, the specimens were processed into sheet-like creep specimens with cross-sectional dimension of 4.5 mm×2.5 mm and gauge length of 20 mm. After mechanical grinding and polishing, the specimens were put into the CTM504A high-temperature creep/rupture testing machine before the creep tests at ultra-high-temperatures. The creep tests were conducted at 1160 °C/120 MPa for 5 and 100 h. The microstructures of the Ni-based superalloys were then observed.

After mechanical grinding and polishing, the etching solution of 5 g CuSO₄, 100 mL HCl, 5 mL H₂SO₄, and 80 mL H₂O was used. The scanning electron microscopy (SEM, S3400) was used to observe the specimen morphologies. The specimens after creep for different durations were analyzed by the transmission electron microscopy (TEM). The film specimens for TEM observation was 3 mm in length and about 60 μm in thicknesses. At -20 °C, an electrolyte of 7vol% perchloric acid and 93vol% anhydrous ethanol was used for double spray thinning. The microstructure of the Ni-based superalloy was observed via TEM (TECNAI-G20) to study the deformation mechanism during creep.

2 Results

2.1 Microstructure and creep properties

After the heat treatment, the microstructure on (001) plane of Ni-based superalloy consists of the cubic γ' phase with a size of about 0.4 μm embedded in the γ matrix in a coherent manner, as shown in Fig. 1. The cube with a dark contrast is the γ' phase, which is arranged regularly along the [100] and [010] directions. The white structure along the vertical and horizontal directions is the γ matrix phase. The γ matrix channel has a size of about 0.1 μm.

The γ' phase with fine grain can be observed in the γ matrix, as shown in the rectangular areas in Fig. 1. During the long-term solution treatment at high temperature, the elements are completely dissolved into the matrix. However, during the subsequent cooling and secondary aging treatment at 870 °C, the supersaturation of solute elements Al and Ta causes the precipitation of fine particles of the γ' phase from the matrix which has a cubic morphology and is arranged regularly along

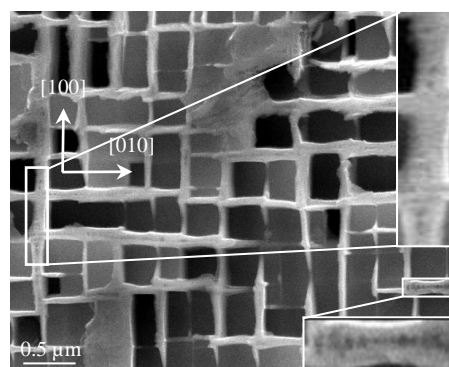


Fig.1 Morphology of 6%Re-5%Ru Ni-based superalloy on (001) plane after entire heat treatment

the [100] and [010] directions^[22].

Fig. 2 shows the creep curve of the Ni-based superalloy after heat treatment and creep at 1160 °C/120 MPa. At the initial stage of creep, the Ni-based superalloy has a large strain, large strain rate, and a short duration. Then the creep of the Ni-based superalloy enters into the steady state stage, where the Ni-based superalloy has a strain rate of 0.0083%/h. The Ni-based superalloy has a creep life of 206 h and a creep fracture strain of 10.96%. Compared with the single-crystal Ni-based superalloy containing 4wt% Re and 4wt% Ru (creep life of 160 h at 1150 °C/100 MPa)^[23], this Ni-based superalloy shows better creep properties at ultra-high temperatures.

Under the applied stress at high temperature, the single-crystal Ni-based superalloy produces an instantaneous strain, which activates the dislocations to propagate rapidly, thereby filling the matrix channels between the cubic γ' phases. With proceeding the creep process, the dislocation density of the Ni-based superalloy is increased. Furthermore, the deformation-hardening effect decreases the strain rate of the Ni-based superalloy. Meanwhile, the thermal activation causes the dislocation glide and dislocation climb, therefore releasing the stress concentration in the local area, and the recovery softening phenomenon occurs. When the deformation

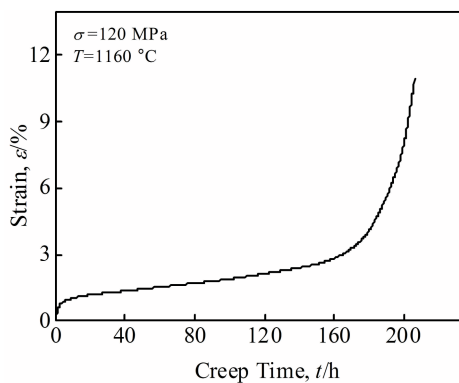


Fig.2 Creep curve of 6%Re-5%Ru Ni-based superalloy at 1160 °C/120 MPa

hardening and recovery softening effects are balanced, the creep of the Ni-based superalloy enters into the steady state stage, where the strain rate of the Ni-based superalloy is fixed, according to Dorn's law^[24].

2.2 Microstructure evolution during creep

When the Ni-based superalloy is heated to 1160 °C, the fine γ' phases in the original heat-treated matrix are completely dissolved, and the cubic γ' phase is regularly arranged along the $\langle 100 \rangle$ direction. SEM morphologies of the loaded area on the (100) crystal plane of the Ni-based superalloy treated at 1160 °C/120 MPa for different durations are shown in Fig. 3. The black area represents the γ' phase, and the gray area is the γ matrix phase. During high-temperature creep, the original cubic γ' phase in the Ni-based superalloy is completely transformed into the raft structure, and its direction is perpendicular to the stress axis. The Ni-based superalloys have different morphologies, sizes, and distortion degrees of the γ' phases due to different creep durations.

After creep for 5 h, the original cubic γ' phase of the Ni-based superalloy is completely transformed into an N-type raft structure perpendicular to the stress axis, as shown in Fig. 3a. Both the γ' raft phase and the γ matrix have the thicknesses of about 0.4 μm . The γ' raft phase is relatively straight, but a few granular γ' phases still exist. Compared with Fig. 1, the area fraction of the γ' raft phase on the (100) plane of Ni-based superalloy is significantly reduced, and more areas are occupied by the sieve-like γ' phase on the (001) plane^[25]. After creep for 100 h, the Ni-based superalloy enters into the steady state stage of creep with the strain of about 2%. Due to the lower strain, the γ' raft phase still retains a relatively straight morphology, but its thickness is increased to 0.6 μm (the thickness of γ matrix is still 0.4~5 μm) due to the coarsening of the γ' phase in the Ni-based superalloy during long-term creep at high temperatures.

After creep for 206 h, due to the necking of the specimen near the fracture, the area under the applied stress is reduced, and the effective stress is further increased, resulting in the coarsening and twisting of the raft phase and increasing the thickness of γ' raft phase to 0.7 μm . When the strain reaches

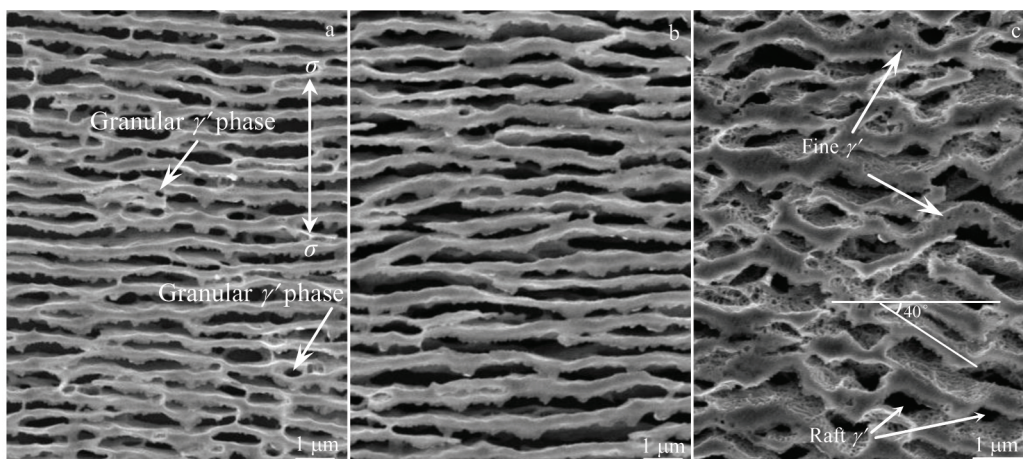


Fig.3 SEM morphologies of Ni-based superalloys after creep at 1160 °C/120 MPa for 5 h (a), 100 h (b), and 206 h (c)

10%, the distortion of γ' raft phase occurs, and the angle between the twisted γ' raft phase and straight γ' raft phase is increased to about 40° , as shown in Fig.3c.

Fig. 4 shows TEM microstructures of the Ni-based superalloy after creep at $1160^\circ\text{C}/120\text{ MPa}$ for different durations. In the area A of Fig.4a, the microstructure changes significantly, and some γ' phases show the raft structure along the direction perpendicular to the stress axis. The γ' raft phase has a thickness of about $0.4\ \mu\text{m}$, but there are still some γ' phases with the granular morphology, as shown in the area B of Fig. 4a, which is in agreement with the results in Fig. 3a. This phenomenon indicates that the element diffusion occurs in the Ni-based superalloy in the initial stage of creep, causing the transformation from the original cubic γ' phase into the raft structure along the direction perpendicular to the stress axis. However, due to the insufficient element diffusion in a short time, some original cubic γ' phases only suffer the corner passivation and are transformed into the spherical shape. In addition, the fine granular γ' phases can be observed in the matrix, as shown in the rectangular area in Fig. 4a, which is formed by the precipitation of supersaturated solute elements from the γ matrix during cooling. In this case, many dislocations are distributed in the γ matrix channel, no dislocations can be observed in the γ' phase, and the γ' phase is sheared by only a few dislocations.

After creep for 100 h, the Ni-based superalloy is in the steady state stage of creep, as shown in Fig.4b. The γ' phase exhibits the N-type raft structure perpendicular to the stress axis. The thickness of the γ' raft phase increases to about $0.65\ \mu\text{m}$. Few dislocations can be observed in the γ' raft phase, but there are many dislocation networks at the γ/γ' interfaces. After creep for 206 h, the γ' phases still retains the raft shape, but the thickness increases to about $0.8\ \mu\text{m}$ in the local area. The area C in Fig.4c reveals that the γ' raft phase is sheared by some dislocations. In the γ matrix, there are many dislocations. The fine granular γ' phases can be observed in the γ matrix channel, as shown in area D in Fig. 4c. In addition, the γ/γ' interface has a large number of dislocation

networks. The rectangular area in Fig.4c shows that the γ' raft phase is sheared by dislocations at the interface. The dislocation network at the interface is damaged because the γ' phase is sheared at the position of the dislocation network. The shear dislocations are along $[01\bar{1}]$ and $[011]$ directions at 45° to the stress axis and suffer the maximum shear stress of the applied load. These phenomena occur in the late stage of creep, and the Ni-based superalloy is considered to lose creep resistance in this area at this stage.

2.3 Contrast analysis of dislocation configuration

After creep for 206 h at $1160^\circ\text{C}/120\text{ MPa}$, the morphologies far from fracture area are shown in Fig. 5. The dislocations with the similar shapes along the trace direction parallel to $[020]$ direction are marked by E, and other groups of dislocations along the same trace direction are marked as $F_1\sim F_4$. F_4 indicates the dislocation loop with an extension direction of $[020]$. In addition, the dislocations with mutually perpendicular traces are denoted as G_1 and G_2 , and their trace directions are parallel to the $[022]$ and $[02\bar{2}]$ directions, respectively. The trace direction of dislocation H is $\mu_H=[002]$.

Fig. 5a shows that when the diffraction vector is $g=[020]$, the dislocations E, $F_1\sim F_4$, and H display a contrast, whereas the dislocations G_1 and G_2 disappear. Based on the invisibility criterion of dislocations, the Burgers vectors of dislocations G_1 and G_2 are determined as $b_{G_1}=b_{G_2}=a[101]$, and their trace directions are $\mu_{G_1}=[022]$ and $\mu_{G_2}=[02\bar{2}]$, respectively. Therefore, the $(11\bar{1})$ plane and (111) plane are the glide planes of the dislocations G_1 and G_2 , respectively. Fig. 5c indicates that when the diffraction vector is $g=[311]$, the dislocations G_1 and G_2 display a contrast, and dislocations E and $F_1\sim F_4$ disappear. Based on the invisibility criterion of dislocations, the Burgers vectors of dislocations E and $F_1\sim F_4$ are determined as $b_E=b_F=a[01\bar{1}]$, and their trace directions are $\mu_E=\mu_F=[020]$. Hence, the glide planes of dislocations E and $F_1\sim F_4$ are $b_E\times\mu_E=b_F\times\mu_F=(100)$. In addition, the dislocation E in the rectangular area in Fig. 5b shows a double line contrast (denoted as dislocation E_1), which is caused by the dislocation decomposition. The analysis shows that the $a[01\bar{1}]$ dislocations

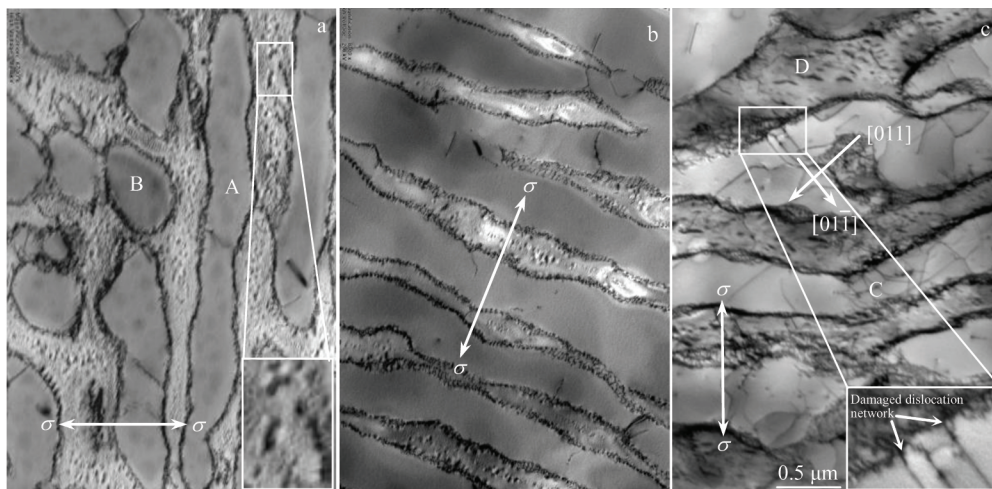


Fig.4 TEM microstructures of Ni-based superalloys after creep at $1160^\circ\text{C}/120\text{ MPa}$ for 5 h (a), 100 h (b), and 206 h (c)

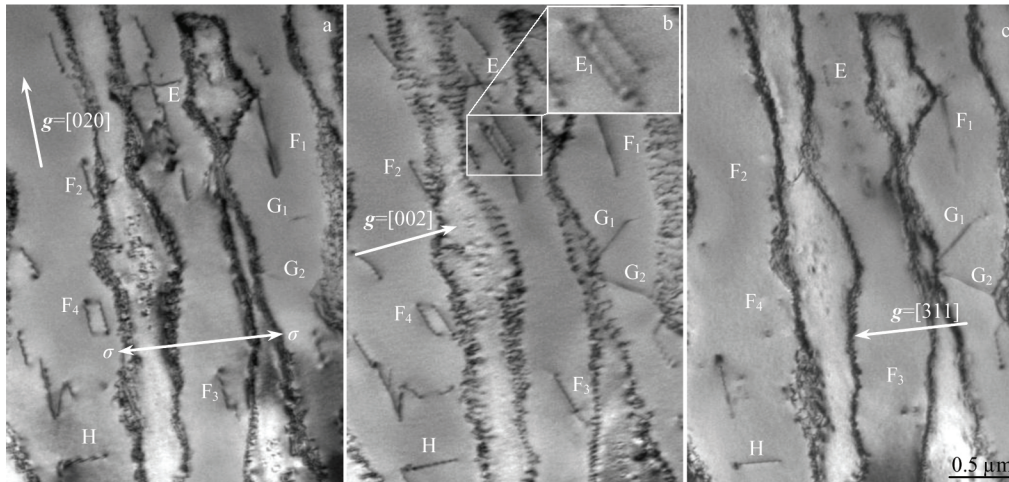


Fig.5 Dislocation configurations of γ' raft phase after creep for 206 h at 1160 °C/120 MPa based on different diffraction vectors: (a) $g=[020]$, (b) $g=[002]$, and (c) $g=[311]$

activated during creep firstly glide on the $\{111\}$ plane. When the dislocation glide is blocked, the cross-slip dislocation occurs from the $\{111\}$ plane to the $\{100\}$ plane and then the dislocations decompose on the (100) plane to form the $(a/2)[01\bar{1}]$ incomplete dislocation. There is an APB between the two incomplete dislocations, as shown in the rectangular area in Fig. 5b. The expression of the decomposition reaction can be described as follows:

$$a[01\bar{1}]_E = (a/2)[01\bar{1}]_{E_1} + (\text{APB})_{(100)} + (a/2)[01\bar{1}]_{E_2} \quad (1)$$

Other dislocations E and $F_1 \sim F_4$ all glide on the (100) plane and show single line contrast because they do not decompose. When the diffraction vectors $g=[020]$, $g=[002]$, and $g=[311]$, the dislocation H show a contrast in Fig. 5a, 5b, and 5c, respectively. The trace direction of dislocation H is $\mu_H=[002]$. Therefore, the Burgers vector of dislocation H can be uniquely determined as $b_H=a[011]$, and the glide plane is $b_H \times \mu_H = (100)$.

Therefore, the deformation mechanism of the 6%Re-5%Ru Ni-based superalloy in the late stage during ultra-high-temperature creep is that the γ' phase is sheared by the dislocation glide in the matrix on the $\{111\}$ plane or the $\{100\}$ plane. The dislocations on the $\{100\}$ plane all originate from the cross-slip of the $\{111\}$ plane^[16]. The plane-angle cross-slip dislocation from the $\{111\}$ plane to the $\{100\}$ plane is regarded as the K-W dislocation lock, which is a fixed dislocation with the ability to inhibit the dislocations from glide and cross-slip and to enhance the creep resistance of the Ni-based superalloy. During the creep at 1160 °C, the cross-slip from the $\{111\}$ plane to the $\{100\}$ plane still occurs and then the dislocations decompose. Thus, the incomplete dislocation+APB configuration cannot be formed or even retained. It can be found that the number of dislocations gilding on the $\{111\}$ plane is less than that on the $\{100\}$ plane, and the dislocations on the $\{100\}$ plane are all K-W dislocation locks formed by the cross-slip from $\{111\}$ plane. Since the Ni-based superalloy can still form and retain a large number of K-W dislocation lock configurations during creep at 1160 °C, the good creep resistance of the Ni-based

superalloy remains.

In the late stage of creep, the high-density dislocations accumulated in the matrix of the Ni-based superalloy cause damage to the dislocation networks on the γ/γ' interface, as shown in Fig. 4c. The stress concentration in the high-density dislocation area can cause the dislocations in the matrix to shear the γ' phase in the damaged dislocation network area. As the creep proceeds, the dislocations suffer the bidirectional cross-slip along the direction of the largest shear stress under the maximum shear stress of the applied load, as shown in Fig. 5c. In particular, the bidirectional cross-slip dislocations activated by the creep dislocations can cause the distortion of γ/γ' raft phases in the Ni-based superalloy, leading to the crack initiation at the distorted interface. With further proceeding the creep process, the strain of Ni-based superalloy is increased and the cracks on the twisted γ/γ' interface are further expanded along the direction perpendicular to the stress axis. Mutual connection of the crack propagation of different cross-sections via the tearing edge can cause the creep fracture of the Ni-based superalloy^[26,27].

3 Discussion

3.1 Hindrance of dislocation movement

In the early stage of ultra-high-temperature creep, the transformation from the cubic γ' phase in the Ni-based superalloy into an N-type raft structure occurs. Fig. 4b indicates that as the creep enters into the steady state stage, the phenomenon of γ' raft phase being sheared by dislocations in the Ni-based superalloy does not happen. Meanwhile, the dislocation climb over the γ' raft phase mainly contributes to controlling the strain rate in the steady state creep.

During the ultra-high-temperature creep, several effects hinder the dislocation movement in the Ni-based superalloy matrix: (1) the effect of the stress field produced by the high density of adjacent dislocations in the matrix (τ); (2) the barrier effect of the lattice distortion caused by the heavy atoms with large radius and Re groups dissolved in the matrix

(τ). Through the combination of applied stress at high-temperature and thermal activation, the dislocation glide and dislocation climb are promoted, which proceeds the creep of the Ni-based superalloy. The force applied on the dislocation line during creep is denoted as $f(x)$, where x denotes the dislocation glide distance. The external force is $f = \tau_R b l$, where $\tau_R = \tau_i + \tau$, b is the Burgers vector of the dislocation, and l is the length of dislocation line. When a thermal activation causes a dislocation to glide from position x_1 to x_2 and cross the barrier, the free energy change (ΔG) of the system can be expressed as follows^[28]:

$$\Delta G = \int_{x_1}^{x_2} [f(x) - \tau b l] dx = \Delta F - \tau_c b \Delta a \quad (2)$$

where x_1 and x_2 are the starting and ending positions of the dislocation glide, τ is the external stress, τ_c is the effective stress, $\Delta F = \int_{x_1}^{x_2} [f(x) - \tau b l] dx$ is the energy required for the dislocation to cross the barrier, and $\Delta a = l \Delta x$ is the area swept by the dislocation during the thermal activation process, namely activation area. The term $\tau_c b \Delta a$ in Eq.(2) represents the energy provided by the effective stress. Thus, the strain rate of the Ni-based superalloy deformation caused by the dislocation glide can be expressed as follows:

$$\dot{\epsilon} = \dot{\epsilon}_0 \exp\left(-\frac{\Delta G}{RT}\right) = \dot{\epsilon}_0 \exp\left(-\frac{\Delta F - \tau_c b \Delta a}{RT}\right) \quad (3)$$

where $\dot{\epsilon}_0 = b \rho_m \lambda v_0$, λ is the distance between obstacles, ρ_m is the dislocation density, v_0 is the vibration frequency of the dislocation, T is the thermodynamic temperature, and R is the Boltzmann constant. It can be concluded from Eq.(3) that the increase in temperature causes the gradual dissolution of fine γ' phases in the Ni-based superalloy, the increase in spacing λ of the fine γ' phases, the decrease in dislocation density, and the increase in strain rate of the Ni-based superalloy.

3.2 Theoretical analysis of effect of Re/Ru addition on creep resistance

In the single-crystal nickel-based alloys, there are two phases with face-centered cubic (fcc) structure: the γ and the γ' phases. The dislocations activated during creep firstly glide on the $\{111\}$ plane. There are dislocations on the $\{100\}$ plane of the Ni-based superalloy during ultra-high-temperature creep, suggesting that the dislocations in the γ' phase can glide from the $\{111\}$ plane to the $\{100\}$ plane, i.e., the cross-slip occurs,

and decomposes to form the K-W dislocation lock+APB configuration, as indicated by the dislocations $F_1 \sim F_4$ in Fig. 5. The K-W dislocation lock and K-W dislocation lock+APB configurations can hinder the dislocation glide and cross-slip dislocation, thereby enhancing the deformation resistance of Ni-based superalloy. However, the thermal activation can cause the dislocation in the K-W dislocation lock to glide again on the $\{111\}$ plane. So the dislocation in the K-W dislocation lock can be released. Therefore, with increasing the temperature, the retention of K-W dislocation locks in the γ' phase is crucial for the Ni-based superalloy to maintain the good creep resistance.

Fig.6a shows the schematic diagram of the γ' phase of rich-Re and rich-W being sheared by dislocations and the formation of K-W dislocation lock through the cross-slip from the $\{111\}$ plane to the $\{100\}$ plane, as indicated by the step 1, step 2, and step 3 in order.

Under the stress field in ultra-high-temperature creep, the element diffusion and dislocation movement may occur simultaneously in the γ/γ' phases. The refractory atoms, such as W, Mo, Re, and Ru, dissolved in the γ' phase are precipitated in the γ/γ' interface^[29] under high temperature and applied load, as denoted by the dotted circles in Fig.6a, which delays the element diffusion rate. During the ultra-high-temperature creep, the refractory atoms assembled near the interface can enter the γ matrix. In addition, the Ni-based superalloy suffers the plastic deformation during creep, causing many dislocations to shear the γ' phase along the $\{111\}$ plane, as shown by the step 1 and step 2 in Fig.6a. With proceeding the creep and element diffusion, the γ/γ' interface moves to the side of the γ' phase, and the W, Mo, Re, and Ru atoms on the $\{111\}$ plane of the γ' phase hinder the dislocation glide on the $\{111\}$ plane. Thus, the cross-slip in the γ' phase from the $\{111\}$ plane to the $\{100\}$ plane occurs, forming the K-W dislocation lock, as shown by the step 2 and step 3 in Fig.6a.

During the ultra-high-temperature creep, the hindrance of dislocations in the γ matrix moving to the γ/γ' interface is improved, as the number of refractory elements remaining in the interface increases, as shown in Fig.6b. With proceeding the creep, many dislocations are stacked next to the γ/γ' interface, thereby generating the stress concentration, which

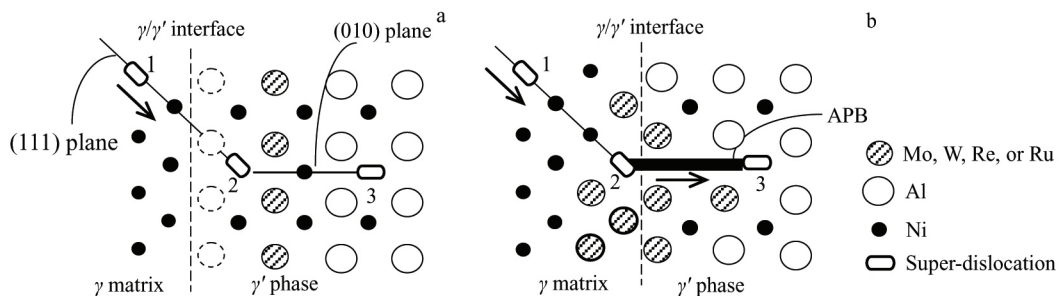


Fig.6 Schematic diagrams of cross-slip dislocations from $\{111\}$ plane to $\{100\}$ plane (a) and dislocation decomposing on $\{100\}$ plane before forming K-W dislocation locks+APB (b)

promotes the dislocations to shear the γ' phase and releases the stress concentration in the interface region^[30]. Because the Re and W atoms in the γ' phase hinder the dislocation movement, the cross-slip from the $\{111\}$ plane to the $\{100\}$ plane occurs and the dislocations decompose before forming the APB, as shown in Fig.6b. Because the formed APB can also inhibit the dislocation movement, the critical shear stress ($\Delta\tau$) for hindering the dislocation movement and for preventing the γ' phase being shearing can be expressed as follows:

$$\Delta\tau = \frac{B\mu(\Delta\delta)}{b} \left(\frac{c_T r f \eta_{APB}}{t} \right)^{1/2} \quad (4)$$

where B is a constant related to the dislocation type ($B=3$ corresponds to edge dislocation; $B=1$ corresponds to screw dislocation), μ is the shear modulus, b is the Burgers vector of the dislocation, $\Delta\delta$ is the mismatch degree, η_{APB} represents the APB energy per unit area, t is the dislocation line tensor, r is the size of γ' phase, f is the volume fraction of γ' phase, and c_T is the content of refractory element. According to Eq.(4), $\Delta\tau$ is increased as the size of the γ' phase, the volume fraction of the γ' phase, and the content of refractory element are increased. Due to the high volume fraction of the γ' phase and the high content of the refractory elements, the 6%Re-5%Ru Ni-based superalloy retains good creep resistance under ultra-high-temperature condition of 1160 °C/120 MPa.

4 Conclusions

1) The single-crystal nickel-based superalloy containing 6wt% Re and 5wt% Ru has good creep resistance at ultra-high temperatures. The deformation mechanism during steady state creep is the dislocation glide in the matrix and the dislocation climb over the γ' raft phase.

2) The interaction of Ru with Re and W elements in the Ni-based superalloy with high content of Re and Ru causes a large number of Re and W atoms to dissolve into the γ' phase, which delays the element diffusion rate and hinders the dislocation movement. This is the main reason that the Ni-based superalloys can retain a large number of Kear-Wiltsdorf (K-W) dislocation locks during the creep at 1160 °C, therefore remaining the good creep resistance of Ni-based superalloy.

References

- 1 Tian S G, Zeng Z, Zhang C et al. *Rare Metal Materials and Engineering*[J], 2013, 42(3): 464
- 2 Nystrom J D, Pollock T M, Murphy W H et al. *Metallurgical and Materials Transactions A*[J], 1997, 28(12): 2443
- 3 Su Xianglin, Sun Changbo, Xu Qingyan et al. *Rare Metal Materials and Engineering*[J], 2017, 46(12): 3699 (in Chinese)
- 4 Shi C X, Zhong Z Y. *Acta Metallurgica Sinica*[J], 1997, 33(1): 1
- 5 Geng C Y, Wang C Y, Yu T. *Acta Materialia*[J], 2004, 52(18): 5427
- 6 Liu S H, Liu C P, Ge L et al. *Scripta Materialia*[J], 2017, 138: 100
- 7 Liao J H, Bor H Y, Chao C G et al. *Materials Transactions*[J], 2010, 51(4): 810
- 8 Tian S G, Wang M G, Li T et al. *Materials Science & Engineering A*[J], 2010, 527(21-22): 5444
- 9 Du Yunling, Niu Jinping, Wang Xinguang et al. *Rare Metal Materials and Engineering*[J], 2018, 47(4): 1248 (in Chinese)
- 10 Wang Y J, Wang C Y. *Materials Science & Engineering A*[J], 2004, 490(1-2): 242
- 11 Yeh A C, Sato A, Kobayashi T et al. *Materials Science & Engineering A*[J], 2008, 490(1-2): 445
- 12 Muller L, Glatzel U, Felle-Kniemeier M. *Acta Metallurgica et Materialia*[J], 1992, 40(6): 1321
- 13 Heckl A, Neumeier S, Göken M et al. *Materials Science & Engineering A*[J], 2011, 528(9): 3435
- 14 Cairney J M, Rong T S, Jones I P et al. *Philosophical Magazine* [J], 2003, 83(15): 1827
- 15 Tian S G, Zhang B S, Shu D L et al. *Materials Science & Engineering A*[J], 2015, 643: 119
- 16 Kear B H, Wiltsdorf H G F. *Transactions of the American Institute of Mining, Metallurgical and Petroleum Engineers*[J], 1962, 224(2): 382
- 17 Hobbs R A, Zhang L, Rae C M F et al. *Materials Science & Engineering A*[J], 2008, 489(1-2): 65
- 18 Zhao G Q, Tian S G, Zhang S K et al. *Progress in Nature Science: Materials International*[J], 2019, 29(2): 210
- 19 Jin Tao, Zhou Yizhou, Wang Xinguang G et al. *Acta Metallurgica Sinica*[J], 2015, 51(10): 1153 (in Chinese)
- 20 Zhang J X, Murakumo T, Koizumi Y et al. *Metallurgical & Materials Transactions A*[J], 2004, 35(6): 1911
- 21 Hegde S R, Kearsey R M, Beddoes J C. *Materials Science & Engineering A*[J], 2010, 527(21-22): 5528
- 22 Zhao G Q, Tian S G, Shu D L et al. *Materials Research Express* [J], 2020, 7(6): 66 507
- 23 Tan X P, Liu J L, Jin T et al. *Materials Science & Engineering A* [J], 2013, 580: 21
- 24 Feng Q, Nandy T K, Pollock T M. *Materials Science & Engineering A*[J], 2004, 373(1-2): 239
- 25 Tian S G, Zhou H H, Zhang J H et al. *Materials Science and Technology*[J], 2000, 16(4): 451
- 26 Tian S G, Ding X, Guo Z G et al. *Materials Science & Engineering A*[J], 2014, 594: 7
- 27 Zhang J X, Murakumo T, Koizumi Y et al. *Journal of Materials Science*[J], 2003, 38(24): 4883
- 28 Zhang Junshan. *High Temperature Deformation and Fracture of Materials*[M]. Beijing: Science Press, 2004: 23 (in Chinese)
- 29 Yan H J, Tian S G, Zhao G Q et al. *Materials Science & Engineering A*[J], 2019, 768: 138 437
- 30 Yang H, Li Z H, Huang M S. *Computational Materials Science* [J], 2013, 75: 52

单晶镍基高温合金超高温蠕变期间的变形机制

赵国旗^{1,2}, 田素贵¹, 刘丽荣¹, 田宁², 晋芳伟²

(1. 沈阳工业大学 材料科学与工程学院, 辽宁 沈阳 110870)

(2. 贵州工程应用技术学院 机械工程学院, 贵州 毕节 551700)

摘要: 通过蠕变性能测试及组织形貌观察, 研究了6%Re-5%Ru (质量分数) 单晶镍基高温合金的超高温蠕变行为和变形机制。结果表明, 该合金在1160 °C/120 MPa条件下的蠕变寿命为206 h。稳态蠕变期间, 位错在基体中滑移和攀移越过筏状 γ' 相是合金的变形特征, 基体中溶解的高浓度难熔元素可增加位错运动阻力。蠕变后期, 切入筏状 γ' 相的位错可由 $\{111\}$ 面交滑移至 $\{100\}$ 面, 形成Kear-Wilsdorf (K-W) 位错锁, 高数量K-W位错锁可抑制位错滑移和交滑移, 是合金具有较好蠕变抗力和较低应变速率的原因。交滑移可扭曲筏状 γ' 相, 并在两相界面发生裂纹萌生与扩展, 直至断裂, 这是合金蠕变后期的变形与损伤特征。其中, 溶入 γ' 相的Ru原子可替换Al原子, 合金中Ru与Re、W的相互作用使较多的Re、W原子溶入 γ' 相, 延缓元素扩散速率, 阻碍位错运动, 使合金在超高温蠕变期间仍保留高数量K-W位错锁及良好蠕变抗力。

关键词: 单晶镍基合金; 6.0%Re-5.0%Ru; 蠕变; 变形机制; K-W位错锁

作者简介: 赵国旗, 男, 1986年生, 博士, 沈阳工业大学材料科学与工程学院, 辽宁 沈阳 110870, 电话: 024-25496785, E-mail: zhaoguoqi1986@163.com